Polymer Chemistry

Accepted Manuscript

This is an *Accepted Manuscript*, which has been through the Royal Society of Chemistry peer review process and has been accepted for publication.

Accepted Manuscripts are published online shortly after acceptance, before technical editing, formatting and proof reading. Using this free service, authors can make their results available to the community, in citable form, before we publish the edited article. We will replace this *Accepted Manuscript* with the edited and formatted *Advance Article* as soon as it is available.

You can find more information about *Accepted Manuscripts* in the Information for Authors.

Please note that technical editing may introduce minor changes to the text and/or graphics, which may alter content. The journal's standard Terms & Conditions and the Ethical guidelines still apply. In no event shall the Royal Society of Chemistry be held responsible for any errors or omissions in this *Accepted Manuscript* or any consequences arising from the use of any information it contains.

ROYAL SOCIETY OF CHEMISTRY

www.rsc.org/polymers

Journal Name

ARTICLE

Molecularly-Defined Macrocycles Containing Azobenzene Main-Chain Oligomers: Modular Stepwise Synthesis, Chain-Length and Topology-Dependent Properties

Received 00th January 20xx,
Accepted 00th January 20xx

DOI: 10.1039/x0xx00000x

www.rsc.org/

Xi Jiang, [a] Jinjie Lu, [a] Feng Zhou, [a] Zhengbiao Zhang, [a] Xiangqiang Pan, [a] Wei Zhang, [a] Yong Wang, [b] Nianchen Zhou,* [a] Xiulin Zhu* [a]

The synthesis and properties of macrocyclic structures have attracted continuous attention since that the cyclic topology effect may offer unique performance. As is well-known, the properties of polymers/oligomers are dependent on molecular weight (chain length). Therefore, the precision synthesis of molecularly-defined macrocycles is doubtlessly a prerequisite to precisely explore the structure-property relationship. Herein, a series of molecularly-defined macrocycles with main-chain azobenzene-containings oligomers (six generation) is prepared efficiently, based on click chemistry and stepwise chain-growth strategy. The cyclic topology and chain-length effects on the properties/functions of the cyclic oligomers are investigated elaborately by comparison with the linear analogues. This work undoubtedly illustrates an example for demonstrating properties/functions dependent on both cyclic topology and chain-length, allowing the in-depth insight into the structure-property relationship. Moreover, the current modular strategy can be extended to various molecularly-defined macrocycles with a wide variety of functions.

Introduction

As we know, the properties and functions of polymers/oligomers are dependent on molecular weight (chain length) and chemical structures; and the molecular weights of polymers/oligomers are polydisperse arising from intrinsic synthesis route. Therefore, it is hard to obtain precise insight into the dependence of physical properties on chain length and chemical structure. As a consequence, the precision synthesis of polymers with molecularly-defined chain lengths (*i.e.*, monodisperse molecular weight), chemical structures, and topologies is a prerequisite. Generally, there are two approaches for the step-wise construction of monodisperse polymers or oligomers with dendritic, linear or cyclic polymer chains.[1] The first one is stepwise chain-growth approach.[1e, 1g] The second one is the "geometrical approach",[1b-1d] by which yields the sequence of length 2^n for n repeat cycles. To investigate the chain-length dependent properties, the stepwise chain-growth approach is undoubtedly the primary choice, since that monomer repeat unit propagates *via* the one-by-one mode.

Besides chain length, the polymeric topologies usually impose significant impacts on the properties and functions of polymers. Notably, the cyclic polymers often display unique performance compared with their *linear* precursors owing to its chain-end free topology. During the past years, cyclic polymers have aroused more and more interests because of its fantastic and interesting functions.[2] Considering the effects from chain length and cyclic topology, the molecularly-defined cyclic polymer was envisioned to provide good model for precisely exploring the structure-property relationship.[1f-1g]

Up to date, diverse azobenzene-based materials have exhibited unparalleled functions and wide application in optical materials, photo-controlling biomolecules and self-organized nanostructures, owning to the unique *cis-trans* photoresponsive performance of azobenzene.[3] Furthermore, towards good performance, azobenzene-containing polymers with different architectures have been well tailored and documented.[4] Impressively, when one or multiple azobenzene moieties are incorporated in a cyclic structure, the topological

[a] State and Local Joint Engineering Laboratory for Novel Functional Polymeric Materials, Jiangsu Key Laboratory of Advanced Functional Polymer Design and Application; Suzhou Key Laboratory of Macromolecular Design and Precision Synthesis; College of Chemistry, Chemical Engineering and Materials Science, Soochow University, Suzhou 215123, China. E-mail: xlzhu@suda.edu.cn, nczhou@suda.edu.cn
[b] Key Laboratory of Organic Synthesis of Jiangsu Province College of Chemistry, Chemical Engineering and Materials Science, Soochow University, Suzhou 215123, P. R. China.
† Electronic Supplementary Information (ESI) available. See
DOI: 10.1039/x0xx00000x

constraint imposed by ring strain can trigger much larger impact on photoswitching properties of azobenzene, and thus the cyclic compounds have display unique and superior functions contrasting to non-cyclic structures.[5a-5d, 6] The emergence of cyclic azobenzene-containing compounds has provided an additional opportunity to develop most versatile materials including chiroptical switches, liquid-crystal displays, responsive nanopores, fluorescence emission, surface relief gratings and so on.[5e-5i, 6]

Herein, we report a series of molecularly-defined cyclic oligomers with alternant tetraglycol (TEG) and azobenzene moieties main chain, based on click chemistry and stepwise chain growth strategy, as shown in Scheme 1&2. By comparison with the linear analogues, the topology and chain-length effects on the photo-responsive behavior of azobenzene are investigated systematically. This work undoubtedly illustrates an example for demonstrating properties/functions dependence on both cyclic topology and chain-length, allowing the in-depth insight into the structure-property relationship and finally enriching the research of azobenzene-derived polymers.

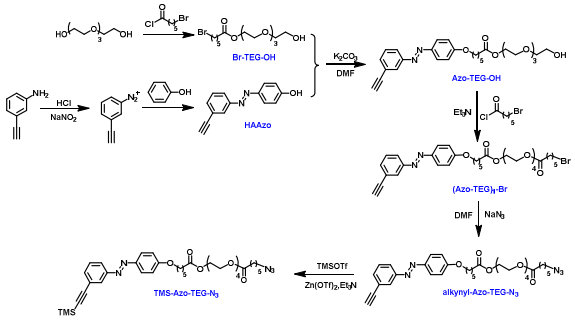

Scheme 1. The synthetic routes of monomer TMS-Azo-TEG-N_3 in the stepwise chain-growth approach

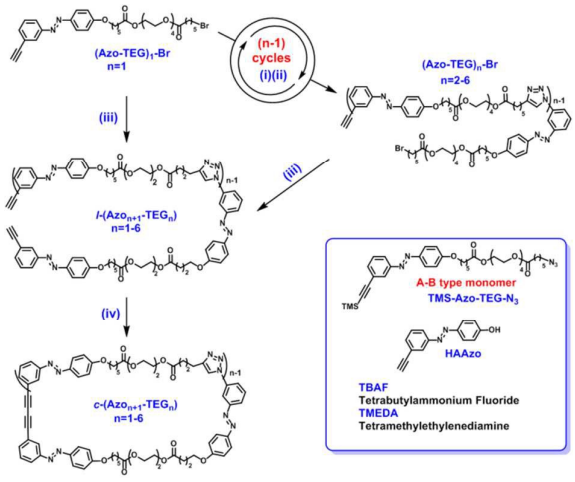

Scheme 2. The synthetic routes of the molecularly-defined linear and cyclic oligomers, *l*-(Azo_{n+1}-TEG_n) and *c*-(Azo_{n+1}-TEG_n) (n=1-6), containing azobenzene main-chain *via* modular stepwise chain-growth approach. (i) stepwise chain-growth via CuAAC click chemistry of TMS-Azo-TEG-N_3: CuBr, PMEDTA, DCM; (ii)TMS deprotection: TBAF; (iii) Williamson reaction: HAAzo, K_2CO_3, KI, DMF; (iv) intramolecular Glaser coupling reaction: CuI, TMEDA,Et_3N, acetone.

Experimental

Materials

N, N, N′, N″, N‴-Pentamethyldiethylenetriamine (PMDETA; 98%; J&K) was dried with 4 Å molecular sieves and distilled under vacuum. Copper (I) bromide (CuBr; chemical pure) was purified *via* washing with acetic acid, water and ethanol, and then dried in vacuum. Tretraethylene glycol (TEG; 99.2%, J&K), 3-ethynylaniline (>98%; Aldrich), *N,N,N′,N′*-Tetramethylethylenediamine (TMEDA; 99%, Energy Chemical), sodium azide (≥99.5%; Aldrich), copper (I) iodide (CuI; chemical pure), tetrabutylammonium fluoride (TBAF; 1.0 mol/L in tetrahydrofuran (THF), Energy Chemical), Zinc trifluoromethanesulfonate ($Zn(OTf)_2$; 98%, TCI), trimethylsilyl trifluoromethanesulfonate (TMSOTf; 99%, Energy Chemical), triethylamine (TEA; analytical reagent) were used as received. Unless otherwise specified, all chemicals were purchased from Shanghai Chemical Reagent Co. Ltd., Shanghai, China.

Characterization

Proton nuclear magnetic resonance (^{1}H NMR) spectra of the samples were recorded on a Bruker nuclear magnetic resonance instrument (300 MHz) using tetramethylsilane (TMS) as the internal standard at room temperature. ^{1}H NMR spectrum of the 3'-ethynylphenyl(4-hydroxy)azobenzene (HAAzo) was recorded on a Varian Inova 400 MHz NMR instrument.The number-average molecular weight (M_n) and molecular weight distribution (M_w/M_n) of the samples were determined by a TOSOH HLC-8320 gel permeation chromatograph (GPC) equipped with refractive-index and UV detectors, using two TSKgel Super Mutipore HZ-N (3 μm beads size) columns arranged in series with a separating molecular weight ranging from 500 to 190,000 g/mol, calibrated with PS standard samples. THF was used as the eluent at a flow rate of 0.35 mL/min at 40 °C. In order to purify the crude polymers, an Agilent PL-50 preparative GPC system equipped with a manual injector and differential refractive index detector was used. The flow rate was maintained at 3 mL/min and THF was used as the eluent. Separations were achieved using a PL gel 10 μm MIXED-D, 300 × 25 mm preparative GPC column held at 40 °C. The dried crude polymer was dissolved in THF at 15-20 mg/mL concentration and filtered through a 0.45 μm PTFE syringe filter prior to injection. Different fractions were collected manually, and the composition of each was determined using the TOSOH HLC-8320 GPC column as described above.Fourier transform infrared (FT-IR) spectra were recorded on a Bruker TENSOR-27 FT-IR spectrometer.Ultraviolet visible (UV-*vis*) absorption spectra of the samples were determined on a Shimadzu UV-2600 spectrophotometer at room temperature. The fluorescence emission spectra of the samples in dichloromethane (DCM) were obtained on a HITACHI F-4600 fluorescence spectrophotometer at room temperature. Matrix assisted laser desorption/ionization time of flight (MALDI-TOF) mass spectrometry measurement was performed using a UltrafleXtreme MALDI TOF mass spectrometer (Bruker Daltonics) equipped with a 1 kHz smart beam-II laser. The instrument was calibrated, before each measurement, with

specific molecular weight PMMA. The matrix compound trans-2-[3-(4-tert-butylphenyl)-2-methyl-2-propenylidene]-malononitrile (DCTB, Aldrich, >98%) was prepared at a concentration of 20 mg/mL in $CHCl_3$. The sodium trifluoroacetate prepared in ethanol at a concentration of 10 mg/mL was used as cationizing agent. All samples were dissolved in THF at a concentration of about 10 mg/mL.

Synthetic procedures

(A) Synthesis of the monomer TMS-Azo-TEG-N_3: The synthetic route of TMS-Azo-TEG-N_3 is shown in Scheme 1, and detailed synthetic process is as follows.

(a) Synthesis of 3'-ethynylphenyl(4-hydroxy)azobenzene(HAAzo): The HAAzo was synthesized according to the method described in the literature.[6b] The final crude product was purified by column chromatography (silica gel, ethyl acetate/petroleum ether = 1/10) to obtain the HAAzo as yellow solid.

(b) Synthesis of Br-TEG-OH: To a 250 mL three-necked flask, TEG (3.302 g, 17 mmol), freshly distilled DCM (150 mL), and dry TEA (2.091 mL, 15.0 mmol) were respectively added. The solution was stirred in an ice bath. A solution of 6-bromohexanoyl chloride (2.23 mL, 17 mmol) in dry DCM (10 mL) was added dropwise to the mixture at 0-5 °C and then reacted at room temperature for about 4 h. Then deionized water (3×250 mL) was added. The mixture was extracted with DCM (150 mL). The organic layer obtained was dried with anhydrous $MgSO_4$ overnight, filtered, and evaporated in a reduced pressure. The final crude product was purified by column chromatography (silica gel, petroleum ether/ethyl acetate = 3/1) to yield Br-TEG-OH as colorless liquid (3.15g, 50%).

(c) Synthesis of Azo-TEG-OH: A solution of Br-TEG-OH (3.7 g, 10 mmol), HAAzo (6.66 g, 29 mmol), potassium carbonate (2.76 g, 20 mmol), a catalytic amount of potassium iodide, and 50 mL of *N, N*-dimethylformamide (DMF) was prepared in a 100mL round bottom flask. The solution was stirred at 80 °C for 6 h. After cooling to room temperature, deionized water (4×200 mL) was added and the mixture was extracted with ethyl acetate (200 mL). The obtained organic layer was dried with anhydrous $MgSO_4$ overnight, filtered, and evaporated in a reduced pressure. The final crude product was purified by column chromatography (silica gel, petroleum ether/ethyl acetate = 2/1) to yield the Azo-TEG-OH as yellow liquid (4.61 g, 95%).

(d) Synthesis of (Azo-TEG)$_1$-Br: To a 50 mL three-necked flask, Azo-TEG-OH (0.468 g, 0.074 mmol), freshly distilled DCM (15 mL), and dry TEA (0.113 g, 1.121 mmol) were respectively added. The solution was stirred in an ice bath. A solution of 6-bromohexanoyl chloride (0.239 g, 1.121 mmol) in dry DCM (10 mL) was added dropwise to the mixture at 0-5 °C and then reacted at room temperature for about 1.5 h. Then deionized water (3×50 mL) was added. The mixture was extracted with DCM (50 mL). The organic layer obtained was dried with anhydrous $MgSO_4$ overnight, filtered, and evaporated in a reduced pressure. The final crude product was purified by column chromatography (silica gel, petroleum ether/ethyl acetate = 3/1) to yield (Azo-TEG)$_1$-Br as yellow liquid (0.31 g, 97%).

(e) Synthesis of alkynyl-Azo-TEG-N_3: (Azo-TEG)$_1$-Br (0.38 g, 0.551mmol), NaN_3 (0.107 g, 1.653 mmol), and DMF (25 mL) were added into a 50 mL round-bottom flask with a magnetic stirrer, and the reaction mixture was stirred for 24 h at 60 °C. After cooling to room temperature, deionized water (3×50mL) was added and the mixture was extracted with ethyl acetate (50 mL). The organic layer obtained was dried with anhydrous $MgSO_4$ overnight, filtered, and evaporated in a reduced pressure. The final product was collected and dried for 24 h in a vacuum oven (0.38 g, 99%).

Synthesis of TMS-Azo-TEG-N_3: A solution of alkynyl-Azo-TEG-N_3 (0.3265 g, 0.5 mmol), $Zn(OTf)_2$ (0.018 g, 0.05 mmol), trimethylsilyl trifluoromethanesulfonate (TMSOTf) (0.184 mL, 1 mmol), dry TEA (0.155 mL, 1 mmol), and 2 mL dry DCM was prepared in the ampule. The reaction was stirred at room temperature overnight, then quenched with sat NH_4Cl. The mixture was extracted with DCM, whereafter the aqueous layer was extracted three times with DCM, and the organic layer obtained was dried with anhydrous $MgSO_4$ overnight, filtered, and evaporated in a reduced pressure. The final crude product was purified by column chromatography (silica gel, petroleum ether/ethyl acetate = 3/1) to yield TMS-Azo-TEG-N_3 as yellow liquid (0.31 g, 97%). ^{1}H NMR spectrum of TMS-Azo-TEG-N_3 was shown in Figure S1.

(B) Synthesis of *l*-(Azo$_{n+1}$-TEG$_n$) and *c*-(Azo$_{n+1}$-TEG$_n$) (n=1-6) : The synthetic routes of *l*-(Azo$_{n+1}$-TEG$_n$) and *c*-(Azo$_{n+1}$-TEG$_n$) are shown in Scheme 2. Using *l*-(Azo$_{n+1}$-TEG$_n$) and *c*-(Azo$_{n+1}$-TEG$_n$) with n=1 and n=2 as typical samples, the detailed synthetic procedure is as follows. The synthetic approach towards *l*-(Azo$_{n+1}$-TEG$_n$) and *c*-(Azo$_{n+1}$-TEG$_n$) (n=3-6) as well as relevant product purification and characterization are described in details in **Supporting Information**.

(a) Synthesis of *l*-(Azo$_2$-TEG$_1$) and *c*-(Azo$_2$-TEG$_1$) (n=1): A solution of (Azo-TEG)$_1$-Br (0.548 g, 1 mmol), HAAzo (0.444 g, 2 mmol), potassium carbonate (0.552 g, 1 mmol), a catalytic amount of potassium iodide, and 20 mL of DMF was prepared in a 50 mL round bottom flask under vigorous stirring. The solution was stirred at 80 °C for 4 h. After cooling to room temperature, deionized water (3×100 mL) was added and the mixture was extracted with ethyl acetate (200 mL). The organic layer obtained was dried with anhydrous $MgSO_4$ overnight, filtered, and evaporated in a reduced pressure. The final crude product was purified by column chromatography (silica gel, petroleum ether/ethyl acetate = 2/1) to yield the *l*-(Azo$_2$-TEG$_1$) as yellow soft solid (0.824 g, 90.9%).

To a 1000 mL three-necked round-bottomed flask was added acetone (700 mL), CuI (0.955 g, 3.00 mmol), and TMEDA (1.5 mL, 10 mmol), and the solution was stirred for 1 h. The *l*-(Azo$_2$-TEG$_1$) (0.1 mmol, 0.083g) in 20 mL of acetone was added to CuI/TMEDA mixture at room temperature *via* syring pump at rate of 0.4 mL/h. After the addition of polymer solution was completed, the reaction was allowed to proceed for another period of 48 h. The reaction solution was concentrated in a reduced pressure, deionized water (3×500 mL) was added and

the mixture was extracted with ethyl acetate (400 mL) to remove the copper catalyst residues. The organic layer obtained was dried with anhydrous $MgSO_4$ overnight, filtered, and evaporated in a reduced pressure. The final crude product was purified by column chromatography (silica gel, petroleum ether/ethyl acetate = 1/1) to yield *c*-(Azo_2-TEG_1) as yellow soft solid (0.082 g, 95%).

(b) Synthesis of (Azo-TEG)$_n$-Br (n=2-6) *via* iterative CuAAC coupling reaction. Using (Azo-TEG)$_2$-Br (n=2) as typical sample, the detailed synthetic procedure is as follows: A solution of (Azo-TEG)$_1$-Br (1.82 g, 2.5 mmol) in DCM (20 mL) was added to a 50 mL three-necked flask. The mixture was deoxygenated by bubbling with Ar_2 for 0.5 h with stirring at room temperature. Then CuBr (358 mg, 2.5 mmol) and PMDETA (0.58 mL, 2.5 mmol) were charged into the flask under protection of Ar_2. And the solution of TMS-Azo-TEG-N_3 (1.82 g, 0.42 mmol) and DCM (5 mL) was added dropwise into the CuBr/PMDETA reaction mixture. The reaction was allowed to proceed for another period of 1h at room temperature. The mixture was evaporated in a reduced pressure and then purified by column chromatography (silica gel, ethyl acetate) to yield TMS-(Azo-TEG)$_2$-Br as yellow liquid (3.1 g, 95%).

(c) Deprotection of TMS-(Azo-TEG)$_2$-Br: A solution of tetrabutyl ammonium fluoride (TBAF) in THF (0.4 mL, 4 mmol) was added to a solution of TMS-(Azo-TEG)$_2$-Br (3.1 g, 2 mmol) in THF (50 mL) and stirred for 1h at room temperature. Deionized water (3×100 mL) was added and the mixture was extracted with ethyl acetate (200 mL). The organic layer obtained was dried with anhydrous $MgSO_4$ overnight, filtered, and evaporated in a reduced pressure. The final product was collected and dried for 24 h in a vacuum oven (2.68 g, 99%).

(d) Synthesis of *l*-(Azo_3-TEG_2) and *c*-(Azo_3-TEG_2) (n=2): The *l*-(Azo_3-TEG_2) and *c*-(Azo_3-TEG_2) (n=2) were prepared from Azo-TEG)$_2$-Br using the similar procedures as *l*-(Azo_2-TEG_1) and *c*-(Azo_2-TEG_1) (n=1) (The synthetic Procedures are described in **Supporting Information**).

Results and discussion

Synthesis and Characterization of the *l*-(Azo_{n+1}-TEG_n) and *c*-(Azo_{n+1}-TEG_n) (n=1-6)

CuAAC "click" reaction has been proved as the most popular and powerful "click" synthetic reactions.[7] Here, a functionalized A-B type monomer bearing an azide and protected trimethylsilyl (TMS) TMS-alkynyl, consisting of azobenzene and TEG in main-chain, TMS-Azo-TEG-N_3, was designed and synthesized, as shown in Scheme 1. The TMS group was used as an alkynyl-protecting group due to its facile protection-deprotection reactions. Commercially available TEG was chosen as soft building block of polymers for preparing amphiphilic polymers with good solubility. Thereafter, a series of well-defined linear oligomers, (Azo-TEG)$_n$-Br from n=1 to n=6, were prepared *via* iterative CuAAC coupling reaction between (Azo-TEG)$_n$-Br and monomer under mild condition. Then, linear precursors with alkynyl groups at both ends, *l*-(Azo_{n+1}-TEG_n) (n=1-6) were obtained by the Williamson reaction between (Azo-TEG)$_n$-Br and azobenzene-containing unit (HAAzo). Various kinds of well-defined macrocycle oligomers with multiple components can be expected prepare by altering HAAzo structure and the building block of azobenzene and TEG. Finally, the intramolecular cyclization of *l*-(Azo_{n+1}-TEG_n) were carried out to yield cyclic ones, *c*-(Azo_{n+1}-TEG_n) *via* Glaser coupling reaction under highly dilute condition.

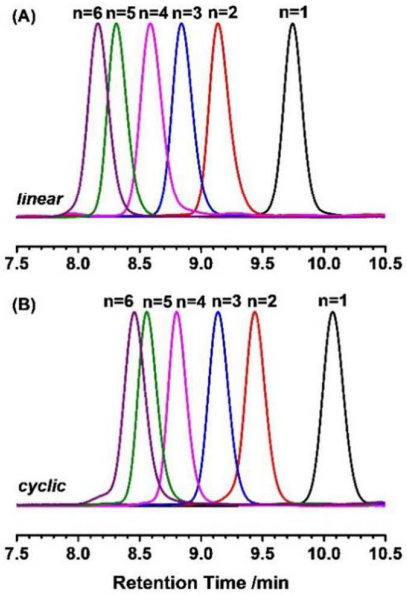

Fig. 1 The GPC trace of *l*-(Azo_{n+1}-TEG_n) (A) and *c*-(Azo_{n+1}-TEG_n) (B) using THF as the eluent (n=1-6).

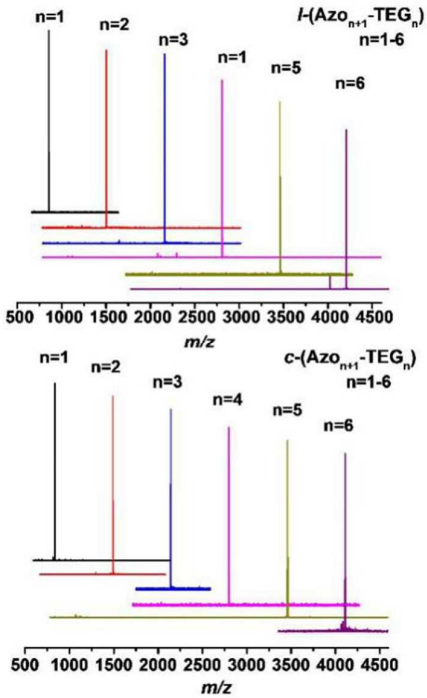

Fig. 2 MALDI-TOF mass spectra of l-(Azo_{n+1}-TEG_n) and c-(Azo_{n+1}-TEG_n) (n=1-6).

The successful preparation of *l*-(Azo_{n+1}-TEG_n) and *c*-(Azo_{n+1}-TEG_n) (n=1-6) and the efficiency of the stepwise chain-growth strategy were verified through comprehensive characterizations including GPC, MALDI-TOF mass spectra, FT-IR measurement and ^{1}H NMR as shown in Figure 1-2, Figures S4-S5 and Table S1. All linear and cyclic products presented unimodal and symmetric GPC traces with narrow molecular weight distributions (M_w/M_n = 1.01-1.05) (Figure 1). Moreover, the cyclic samples show obviously longer elution time compared with linear precursor due to smaller hydrodynamic volumes, which was consistent with the formation of conventional cyclic polymers.[2i, 6] FT-IR spectra (Figure S4) further supported the complete conversion from linear into cyclic ones. Furthermore, the absolute molecular weights and chemical structures of *l*-(Azo_{n+1}-TEG_n) and *c*-(Azo_{n+1}-TEG_n) (n=1-6) were identified by MALDI-TOF mass spectra. As displayed in Figure 2, only a single mass peak was observed, which matched well with the respective calculated molecular weight, showing little or no contamination from failure sequences in all products. The mass peaks obtained from MALDI-TOF mass spectra and molecular weights ($M_{n,\,GPC}$) determined by GPC of linear and cyclic products are summarized in Table S1 for clear illustration. The chemical shifts of protons in *l*-(Azo_{n+1}-TEG_n) and *c*-(Azo_{n+1}-TEG_n) (n=1-6) were monitored by ^{1}H NMR spectra as presented in Figure S5. The signal around 3.13 ppm (j) assigned to the protons of terminal alkynyl groups in linear samples completely disappeared upon the cyclization *via* intramolecular Glaser coupling reaction.[5f]

Photoisomerization of the *l*-(Azo_{n+1}-TEG_n) and *c*-(Azo_{n+1}-TEG_n) (n=1-6)

The photoisomerization performance of the *l*-(Azo_{n+1}-TEG_n) and *c*-(Azo_{n+1}-TEG_n) (n=1-6) were systematically investigated under identical condition. First, the UV-*vis* absorption spectra of the *l*-(Azo_{n+1}-TEG_n) and *c*-(Azo_{n+1}-TEG_n) in DCM were investigated. The representative spectra are shown in Figure 3 using *l*-(Azo_6-TEG_5) and *c*-(Azo_6-TEG_5) (n = 5) as typical samples, and other spectra (n = 1-4 and n = 6) were shown in Figure S6-S10. After the ring closure *via* Glaser coupling, the 1, 3-diynes group is generated, accompanying with the change of the absorption around 260-320 nm of *c*-(Azo_{n+1}-TEG_n).[5f] For *c*-(Azo_{n+1}-TEG_n), the dependence of n, π* transition band on the stepwise chain growth is negligible, while π-π* transition band suffered a blue-shift in contrast to linear oligomers. The evolutions of maximum absorption wavelength ($\lambda_{max,\,trans}$ and $\lambda_{max,\,cis}$) corresponding to *trans*-azobenzene and *cis*-azobenzene with generation (n) growth were plotted in Figure 4. The $\lambda_{max,\,trans}$ of linear products was around 352 nm for all cases, while the $\lambda_{max,\,trans}$ of cyclic ones with n = 1-4 shifted to 351 nm from 338 nm. After ring closure, two azobenzene moieties are connected by 1, 3-diyne in cyclic main chain, cyclic geometries may be thus distorted or deformed because of strain of small ring and steric hindrance induced by the rigid structure. As a result, λ_{max} of the cyclic topologies was changed.[8a] Furthermore, the $\lambda_{max,\,trans}$ of cyclic products shifted to 351 nm when n = 5 and kept unchanged up to n = 6, proving the more obvious restriction effect imposed by small ring. The theoretical calculations on the *c*-(Azo_{n+1}-TEG_n) (n = 1-5) were carried out by using density functional theory (DFT) and employing time-dependent DFT (TDDFT) with the three-parameter hybrid functional (B3LYP) (Supporting Information). Figure S11 shows the plots of the most representative molecular frontier orbital for the *c*-(Azo_{n+1}-TEG_n) (n = 1-5) and summarizes the spin-allowed electronic transitions calculated with the TDDFT method (Figure S11F). The calculated results agree with the experimental ones basically.

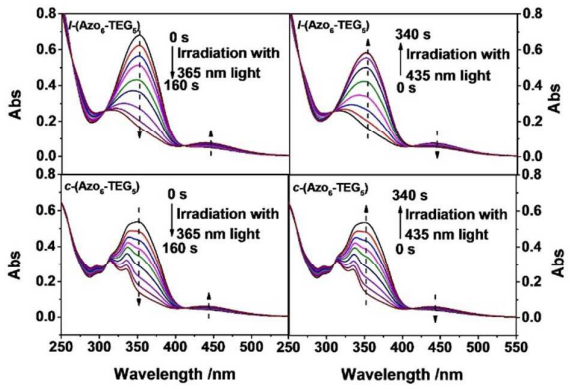

Fig. 3 The UV-*vis* absorption spectra of *l*-(Azo_6-TEG_5) and *c*-(Azo_6-TEG_5) in DCM under irradiation with 365 nm UV light and 435 nm visible light at different time intervals until the photo-stationary were achieved. The concentration of solution is 2.07×10^{-3} mg/mL for both linear and cyclic polymers.

Meanwhile, the solutions of linear and cyclic products were firstly irradiated under 365 nm UV light (light intensity: 0.5 mw cm^{-2}) and then 435 nm light (light intensity: 0.53 mw cm^{-2}) at room temperature, until the photostationary states (PSS_{uv}) of *trans*-to-*cis* and photostationary states (PSS_{vis}) of reverse *cis*-to-*trans* was reached respectively. The related UV-*vis* absorption spectra can be seen from Figure 3 and Figure S6-S10. Further, the first-order kinetic curves of photo-isomerization are plotted in Figure S12, and then the rate constants (k_e and k_H) of *trans-to-cis* isomerization and *cis-to-trans* recovery of linear and cyclic azobenzene products as well as the rate constants ratios (k_e'/k_e and k_H'/k_H) of *c*-(Azo_{n+1}-TEG_n)/ *l*-(Azo_{n+1}-TEG_n) were calculated, as summarized in Table S2. The evolutions of k_e and k_H values with generation (n) growth were plotted in Figure 4. As a whole, the k_e and k_H in linear and cyclic polymers themselves showed no significant change with generation (n). Nevertheless, the cyclic products displayed a distinctly larger k_e value and a slightly larger k_H value, especially at n=1 compared those of linear ones. This result implied that the cyclic topologies had a faster photo-isomerization from *trans*-form to *cis*-form and a slightly faster reversible relaxation from *cis*-isomer to *trans*-isomer, contrasting to linear ones. Two facts might be account for this result. First, as we know, when azobenzene moieties are incorporated into ring skeleton, they generally exhibit faster *trans-to-cis* photo-isomerization due to more stable

conformation for cyclic *cis*-azobenzene relative to the linear analogues, especially for small ring.[6b] Second, compared with the cyclic ones, the linear polymers may be more flexible and more mobility due to absence of strain and presence of swinging chain ends. As a result, the azobenzene groups containing in the linear polymers may suffer more transition resistance of isomerization than cyclic ones.[4a, 9] The first factor was suggested to play a dominating role on the faster *trans*-to-*cis* photo-isomerization for the cyclic products.

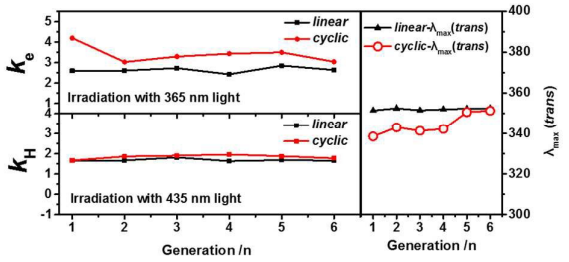

Fig. 4 The evolution of rate constants (k_e and k_H) on generation (n) of *l*-(Azo_{n+1}-TEG_n) and *c*-(Azo_{n+1}-TEG_n) as well as the rate constants ratios of *c*-(Azo_{n+1}-TEG_n)/ *l*-(Azo_{n+1}-TEG_n) (k_e'/ k_e and k_H'/ k_H), n=1-6. The evolution of λ_{max} value of *trans*-azobenzene and *cis*-azobenzene units with generation (n) of *l*-(Azo_{n+1}-TEG_n) and *c*-(Azo_{n+1}-TEG_n), n=1-6.

The percentage of *cis*-azo isomers in the linear ($F_{l\text{-}cis}$) and cyclic oligomers ($F_{c\text{-}cis}$) was calculated quantitatively by the ^{1}H NMR spectra.[8b, 10] The azobenzene moieties of linear and cyclic oligomers for n=1 uniformly presented *trans*-form isomers with the thermodynamic stability. The *cis*-form isomers were generated when azobenzene moieties increased to more than two by increasing generation (n>1), since the polymeric environment around azobenzene moieties induced an influence on the thermal isomerization of azobenzene.[9] The cyclic products from n=2 to n=6 contained about 5.0-7.5 % of $F_{c\text{-}cis}$, which was larger than these of linear one (about 1.0-3.0 % of $F_{l\text{-}cis}$), as shown in Figure S15. The result is supposed that the cyclic geometries might be distorted or deformed by the ring strain and steric hindrance caused by the rigid 1,3-diyne moiety, as a result that the cyclic topology induced more *cis*-form isomers.[8a, 9]

Fluorescence Behavior of the *l*-(Azo_{n+1}-TEG_n) and *c*-(Azo_{n+1}-TEG_n) (n=1-6)

The fluorescence behavior of *l*-(Azo_{n+1}-TEG_n) and *c*-(Azo_{n+1}-TEG_n) in DCM was investigated. The fluorescence emission spectra and their dependent properties on generation (n) are plotted in Figure S16 and S17. Furthermore, the fluorescence quantum yields (Φ_s) of *l*-(Azo_{n+1}-TEG_n) and *c*-(Azo_{n+1}-TEG_n) were determined using quinine sulfate as the standard. The obtained Φ_s values are summarized in Table S3 and plotted in Figure 5. The linear and cyclic products exhibit fluorescence emission centered at around 420 nm. However, no fluorescence was found when further increasing chain length to n = 5 (linear product) or n = 6 (cyclic product), which can be rationalized by the self-quenching effect of intra- or inter-chain fluorescent groups for longer polymeric chain.[11] Overall, the *c*-(Azo_{n+1}-TEG_n) demonstrate fluorescent enhancement relative to linear ones. This result can be attributed to the restricted architectures induced by the cyclic topology, which can enlarge the distance between fluorescent groups, so that the self-quenching effect was depressed.[4a, 5b, 6a]

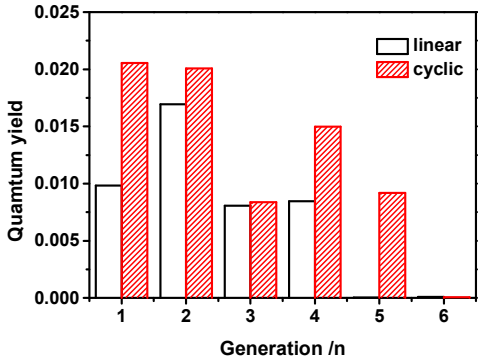

Fig. 5 The evolution of fluorescence quantum yields of *l*-(Azo_{n+1}-TEG_n) and *c*-(Azo_{n+1}-TEG_n) (n = 1-6) with generation (n) in DCM at room temperature. The concentration of solution is 3.6×10^{-8} mol /mL of azobenzene units for both linear and cyclic oligomers. Excitation wavelength: 350 nm.

Conclusions

In summary, a series of molecularly-defined linear and cyclic oligomers containing alternant azobenzene and TEG moieties in main chain, were prepared successfully by the CuAAC "click" chemistry and stepwise chain growth approach. Some investigations on the dependence of functions on chain length and cyclic topology have been evaluated by the comparison of resultant linear and cyclic products. The restricted conformation imposed by the cyclic topology induced an effect on the photosensitive behavior of azobenzene. For example, *c*-(Azo_{n+1}-TEG_n) displayed an obviously faster *trans*-to-*cis* photo-isomerization of azobenzene, a blue shift for π-π* transition band corresponding to *trans*-azobenzene and a fluorescent enhancement compared with those of linear precursors. In addition, some dependence of the properties on the chain length was observed, including progressive change of *cis* isomers percentage, different self-quenching effect of fluorescent emission. These results suggest that the chain length and cyclic topology play an important role on photoresponsive performance of containing-azobenzene compounds. The current modular synthetic strategy can be extended to various molecularly-defined macrocycles with a wide variety of functions. Further investigation on the self-assembly behaviors of the obtained linear and cyclic amphipathic oligomers and synthesis of various smart macrocycles are ongoing in our group.

Acknowledgements

This work was supported by the National Science Foundation of China (21234005, 21574089), the Priority Academic Program Development of Jiangsu Higher Education Institutions

(PAPD) and the Program of Innovative Research Team of Soochow University.

Notes and references

1 (a) M. T. Stone, J. M. Heemstra, J. S. Moore. *Acc. Chem. Res*., 2006, **39**, 11; (b) K. Takizawa, C. Tang, C. J. Hawker. *J. Am. Chem. Soc*., 2008, **130**, 1718; (c) C. J. Hawker, E. E. Malmström, C. W. Frank, J. P. Kampf, *J. Am. Chem. Soc*., 1997, **119**, 990; (d) Q. Wang, Y. Qu, H. Tian, Y. Geng, F. Wang. *Macromolecules,* 2011, **44**, 1256; (e) S. Pfeifer, Z. Zarafshani, N. Badi, J. Lutz. *J. Am. Chem. Soc*., 2009, **131**, 9195; (f) S. Binauld, J. C. Hawker, E. Fleury, E. Drockenmuller. *Angew. Chem. Int. Ed*., 2009, **48**, 6654; (g) V. Percec, P. J. Turkaly, A. D. Asandei. *Macromolecules,* 1997, **30**, 943.

2 (a) M. Schappacher, A. Deffieux. *Science,* 2008, **319**, 1512; (b) L. Li, J. Yang, J. Zhou. *Macromolecules,* 2013, **46**, 2808; (c) M. A. Cortez, W. T. Godbey, Y. Fang, M. E. Payne, B. J. Cafferty, K. A. Kosakowska, S. M. Grayson. *J. Am. Chem. Soc*., 2015, **137**, 6541; (d) D. E. Lonsdale, M. J. Monteiro. *J. Polym. Sci., Part A: Polym. Chem.,* 2011, **49**, 4603; (e) H. Wada, T. Yamamoto, Y. Tezuka. *Macromolecules,* 2015, **48**, 6077; (f) D. Zhang, S. H. Lahasky, L. Guo, C. Lee, M. Lavan. *Macromolecules,* 2012, **45**, 5833; (g) K. Zhang, G. N. Tew. *ACS Macro Lett*., 2012, **1**, 574-; (h) X. Zhu, N. Zhou, Z. Zhang, B. Sun, Y. Yang, J. Zhu, X. Zhu. *Angew. Chem. Int. Ed*., 2011, **50**, 6615; (i) H. R. Kricheldorf. *J. Polym. Sci., Part A: Polym. Chem.,* 2010, **48**, 251.

3 (a) S. Iamsaard, S. J. Aßhoff, B. Matt, T. Kudernac, J. J. L. M. Cornelissen, S. P. Fletcher, N. Katsonis. *Nat. Chem.,* 2014*,* **6***,* 229; (b) O. Sadovski, A. A. Beharry, F. Zhang, G. A. Woolley. *Angew. Chem. Int. Ed*., 2009, **48**, 1484; (c) A. A. Beharry, G. A. Woolley. *Chem. Soc. Rev*., 2011, **40**, 4422; (d) C. Hoppmann, I. Maslennikov, S. Choe, L. Wang. *J. Am. Chem. Soc*., 2015, **137**, 11218; (e) Y. Li, Y. He, X. Tong, X. Wang. *J. Am. Chem. Soc*., 2005, **127**, 2402; (f) Y. Yu, M. Nakano, T. Ikeda. *Nature,* 2003*,* **425**, 145; (g) Y. Zhao, J. He. *Soft Matter*., 2009, **5**, 2686; (h) R. Dong, B. Zhu, Y. Zhou, D. Yan, X. Zhu. *Polym. Chem*., 2013, **4**, 912; (i) K. Han, W. Su, M. Zhong, Q. Yan, Y. Luo, Q. Zhang, Y. Li. *Macromol. Rapid Commun*., 2008, **29**, 1866; (j) H. K. Bisoyi, Q. Li. *Acc. Chem. Res.*, 2014, **47**, 3184; (k) L. Chen, Y. Li, J. Fan, H. K. Bisoyi, D. A. Weitz, Q. Li. *Adv. Optical Mater.,* 2014, **2**, 845; (l) C. Xue, J. Xiang, H. Nemati, H. K. Bisoyi, K. Gutierrez-Cuevas, L. Wang, M. Gao, S. Zhou, D. Yang, O. D. Lavrentovich, A. Urbas, Q. Li. *ChemPhysChem*, 2015, **16**, 1852; (m) R. Sun, C. Xue, X. Ma, M. Gao, H. Tian, Q. Li. *J. Am. Chem. Soc.*, 2013, **135**, 5990; (n) L. Wang, H. Dong, Y. Li, C. Xue, L. Sun, C. Yan, Q. Li. *J. Am. Chem. Soc*., 2014, **136**, 4480.

4 (a) Y. Sun, Z. Wang, Y. Li, Z. Zhang, W. Zhang, X. Pan, N. Zhou, X. Zhu. *Macromol. Rapid Commun.,* 2015, **36**, 1341; (b) Z. Li, G. Yu, P. Hu, C. Ye, Y. Liu, J. Qin, Z. Li. *Macromolecules,* 2009, **42**, 1589; (c) C. Kördel, C. S. Popeney, R. Haag. *Chem. Commun*., 2011, **47**, 6584; (d) E. Blasco, B. V. K. J. Schmidt, C. Barner-Kowollik, M. Piñol, L. Oriol. *Macromolecules,* 2014, **47**, 3693; (e) W. Sun, X. He, C. Gao, X. Liao, M. Xie, S. Lin, D. Yan. *Polym. Chem*., 2013, **4**, 1939.

5 (a) R. Siewertsen, H. Neumann, B. Buchheim-Stehn, R. Herges, C. Näther, F. Renth, F. Temps. *J. Am. Chem. Soc*., 2009, **131**, 15594; (b) J. Yoshino, N. Kano, T. Kawashima, *Chem. Commun*., 2007, **43**, 559; (c) L. Schweighauser, H. A. Wegner. *Chem. Commun.,* 2013, **49**, 4397; (d) R. Reuter, H. A. Wegner. *Chem. Commun.,* 2013, **49**, 146; (e) R. Reuter, H. A. Wegner. *Chem. Commun.,* 2011, **47**, 12267; (f) J. Lu, A. Xia, N. Zhou, W. Zhang, Z. Zhang, X. Pan, Y. Yang, Y. Wang, X. Zhu. *Chem.- Eur. J*., 2015, **21**, 2324; (g) M. Mathews, R. S. Zola, S. Hurley, D. Yang, J. T. White, T. J. Bunning, Q. Li. *J. Am. Chem. Soc*., 2010, **132**, 18361; (h) Y. Norikane, Y. Hirai, M. Yoshida. *Chem. Commun*., 2011, **47**, 1770; (i) C. S. Pecinovsky, E. S. Hatakeyama, D. L. Gin. *Adv. Mater.,* 2008, **20**, 174-178.

6 (a) Y. Zhang, X. Zhu, N. Zhou, X. Chen, W. Zhang, Y. Yang, X. Zhu. *Chem. Asian J.,* 2012, **7**, 2217; (b) J. Li, N. Zhou, Z. Zhang, Y. Xu, X. Chen, Y. Tu, Z. Hu, X. Zhu. *Chem. Asian J*., 2013, **8**, 1095; (c) H. Zhang, N. Zhou, X. Zhu, X. Chen, Z. Zhang, Wei. Zhang, J. Zhu, Z. Hu, X. Zhu. *Macromol. Rapid Commun.,* 2012, **33**, 1845; (d) Y. Cai, J. Lu, F. Zhou, X. Zhou, N. Zhou, Z. Zhang, X. Zhu. *Macromol. Rapid Commun.,* 2014, **35**, 901; (e) B. Chen, Z. Wang, J. Lu, X. Yang, Y. Wang, Z. Zhang, J. Zhu, N. Zhou, Y. Li, X. Zhu. *Polym. Chem.,* 2015, **6**, 3009.

7 H. C. Kolb, M. G. Finn, K. B. Sharpless. *Angew. Chem. Int. Ed.,* 2001, **40**, 2004.

8 (a) Y. Norikane, N. Tamaoki. *Eur. J. Org. Chem.,* 2006, 1296; (b) R. Reuter, H. A. Wegner. *Chem.-Eur. J.,* 2011, **17**, 2987.

9 G. S. Kumar, D. C. Neckers. *Chem. Rev.,* 1989*,* **89***,* 1915.

10 Y. Norikane, R. Katoh, N. Tamaoki. *Chem. Commun*., 2008, 1898.

11 P. Smitha, S. K. Asha. *J. Phys. Chem. B.,* 2007, **111***,* 6364.

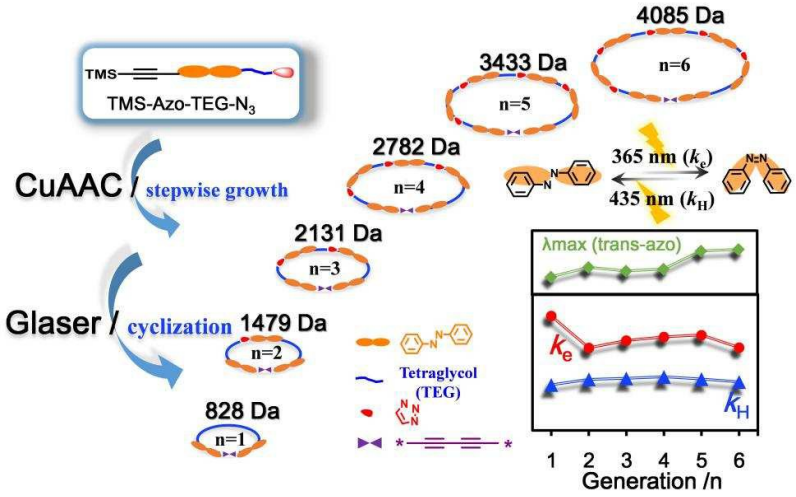

Molecularly-Defined Macrocycles Containing Azobenzene Main-Chain Oligomers: Modular Stepwise Synthesis, Chain-Length and Topology-Dependent Properties

Xi Jiang,[a] Jinjie Lu,[a] Feng Zhou,[a] Zhengbiao Zhang,[a] Xiangqiang Pan,[a] Wei Zhang,[a] Yong Wang,[b] Nianchen Zhou,*[a] Xiulin Zhu*[a]

Molecularly-defined linear and cyclic oligomers with azobenzene main-chain were prepared successfully. And the chain length and cyclic topology induce an effect on photoresponsive performance of the resultant oligomers.